Neoplasia 62 (2025) 101142

Contents lists available at ScienceDirect

Neoplasia

journal homepage: www.elsevier.com/locate/neo

Original Research

O-GlcNAc-modified HOXA9 suppresses ferroptosis via promoting UBR5-mediated SIRT6 degradation in nasopharyngeal carcinoma

Huai Liu [a,b,#], Yingzhou Fu [a,#], Ling Tang [a,b,#], Bo Song [a], Wangning Gu [a], Hongmin Yang [a], Tengfei Xiao [a], Hui Wang [a,b,*], Pan Chen [a,*]

[a] The Affiliated Cancer Hospital of Xiangya School of Medicine, Central South University/Hunan Cancer Hospital, Changsha 410013, China
[b] Key Laboratory of Translational Radiation Oncology, Hunan Province; Department of Radiation Oncology, Hunan Cancer Hospital and The Affiliated Cancer Hospital of Xiangya School of Medicine, Central South University, Changsha 410013, China

ARTICLE INFO

Keywords:
Nasopharyngeal carcinoma
Ferroptosis
HOXA9
UBR5
SIRT6
O-GlcNAcylation

ABSTRACT

Background: Nasopharyngeal carcinoma (NPC) is the most common malignancy of the nasopharynx. Ferroptosis induction shows anti-tumor activities in cancers including NPC. Elucidating the regulatory mechanism of ferroptosis is crucial for developing targeted therapeutic strategies for NPC.
Methods: The GEO dataset (GSE68799) was used to analyze HOXA9 expression in NPC. Cell viability, levels of MDA, total iron, Fe^{2+} and GSH, and lipid peroxidation were examined for ferroptosis evaluation. O-GlcNAcylation levels on HOXA9 and ubiquitination levels on SIRT6 were detected by immunoprecipitation. ChIP and luciferase assays were applied for determining the interaction of HOXA9 and UBR5. The interaction between UBR5 and SIRT6, OGT and HOXA9 were evaluated by Co-IP assays. A subcutaneous NPC mouse model was established to explore whether knockdown of HOXA9 or UBR5 regulates tumor growth *in vivo*.
Results: HOXA9 was highly expressed in NPC, and knockdown of HOXA9 elevated total iron, Fe^{2+} and lipid peroxidation and reduced GSH and NPC cell viability. O-GlcNAcylation stabilized HOXA9 and facilitated its nuclear translocation in NPC cells. HOXA9 directly bound to UBR5 promoter to increase its expression, thus accelerating ubiquitination and degradation of SIRT6. HOXA9 restrained ferroptosis via promoting UBR5 expression, and UBR5 suppressed ferroptosis through promotion of SIRT6 ubiquitination and degradation. Knockdown of HOXA9 or UBR5 promoted ferroptosis and inhibited NPC growth in mice.
Conclusion: O-GlcNAc-modified HOXA9 inhibits ferroptosis by enhancing UBR5 expression and ubiquitination and degradation of SIRT6 in NPC cells, thus accelerating NPC progression. Our study provides potential therapeutic targets for NPC treatment.

Introduction

Nasopharyngeal carcinoma (NPC) is the primary cancer that starts in the nasopharynx. Although it is rare globally, NPC shows obvious geographic prevalence, and highest incidence is observed in Southern China [1]. Thanks to the advancement of therapies such as chemotherapy and intensity-modulated radiation therapy, great improvement has been made in the management of NPC in recent years although drug resistance causes a major obstacle for NPC treatment [2,3]. Unfortunately, approximately 30 % of patients suffer to recurrence and distant metastasis [4], leading to high mortality. Various mechanisms underlying NPC progression have gained much attention [5,6]. Further elucidating underlying mechanisms controlling the progression of NPC is important for identifying novel therapeutic targets.

Ferroptosis, a novel iron-dependent cell death [7], is characterized by lipid peroxidation and serves important roles in various cancers [8–10]. A recent review has discussed potential regulators and mechanisms regulating ferroptosis in sensitizing NPC cells to radiotherapy [11]. It has been reported that triggering ferroptosis inhibits the stemness of NPC cells [12]. Moreover, Huang et al. reported that induction of ferroptosis by cucurbitacin B significantly suppressed the progression of NPC [13]. Liu et al. found that cancer-associated fibroblasts secreted

* Corresponding authors at: Hunan Cancer Hospital and the Affiliated Cancer Hospital of Xiangya School of Medicine, Central South University, No. 283, Tongzipo Road, Yuelu Distirct, Changsha 410031, Hunan Province, PR China.
E-mail addresses: wanghui@hnca.org.cn (H. Wang), chenpan08@csu.edu.cn (P. Chen).
Huai Liu, Yingzhou Fu and Ling Tang are the co-first authors.

https://doi.org/10.1016/j.neo.2025.101142
Received 13 August 2024; Accepted 17 February 2025

FGF5 to suppress ferroptosis to decrease cisplatin sensitivity in NPC by binding to FGFR2 [14]. However, the roles and regulatory mechanisms of ferroptosis in NPC remain to be determined.

Homeobox A9 (HOXA9) is a transcription factor of the HOX protein family and known to regulate hematopoiesis and development [15,16]. Recently, emerging evidence shows that HOXA9 functions as a tumor suppressor or an oncogene in various human cancers. For instance, HOXA9 accelerates the progression of ovarian cancer through activation of cancer-associated fibroblasts [17]. HOXA9 suppresses the development of cutaneous squamous cell carcinoma by inhibiting glycolysis [18]. Intriguingly, a recent study reported elevated expression of HOXA9 in NPC tissues from patients, and high HOXA9 expression indicated poor prognosis in NPC patients [19], suggesting that HOXA9 might act as an oncogene in NPC. Hence, the roles of HOXA9 in the regulation of NPC progression need to be elucidated.

O-GlcNAcylation is a common post-translational modification of proteins that plays key roles in regulating tumor progression. Zhu et al. reported that O-GlcNAcylation promoted the growth of pancreatic cancer by regulating malate dehydrogenase 1 [20]. Moreover, O-GlcNAcylation is an emerging potential mechanism for inducing proliferation, tumor progression and chemotherapy resistance in cancer cells [21]. However, the role of O-GlcNAcylation in NPC is largely unknown. A recent study also has suggested that dynamic O-GlcNAcylation coordinates ferritinophagy and mitophagy to regulate ferroptosis [22]. We identified the presence of O-GlcNAc modification sites in HOXA9 by the YinOYang-1.2 database, and the confidence level was higher than 0.5 at the Thr4 and Ser127 sites, suggesting the implication of O-GlcNAcylation in ferroptosis and NPC.

Sirtuin 6 (SIRT6) belongs to class III histone deacetylase family and plays key roles in DNA damage repair, anti-aging, chromatin regulation and tumor suppression [23]. SIRT6 was reported to be downregulated in NPC cell lines and tissues, and its overexpression enhanced NPC cell apoptosis [24]. Silencing of SIRT6 enhanced the accumulation of reactive oxygen species (ROS), malondialdehyde (MDA) and Fe^{2+} and improved sorafenib chemosensitivity of gastric cancer cells via promoting ferroptosis [25]. On the contrary, Yang et al. found that SIRT6 drove sensitivity to ferroptosis in anaplastic thyroid cancer [26]. Fang and colleagues reported that SIRT6 regulated ferroptosis and prevented glucocorticoid-induced osteonecrosis of the femoral head in rats [27]. Melatonin inhibits ferroptosis through the SIRT6/p-Nrf2/GPX4 and SIRT6/COA4/FTH1 pathways [28]. SIRT6 induces NCOA4-dependent autophagic degradation of ferritin, thus driving sensitivity to ferroptosis [26]. However, we found no significant effect of HOXA9 on SIRT6 mRNA levels by pre-experimentation, whereas analysis of the BioGRID database revealed the presence of multiple post-translational ubiquitination modification sites in SIRT6 and binding relationships with multiple E3 ubiquitination ligases including UBR5.

Ubiquitin protein ligase E3 component n-recognin 5 (UBR5) is a highly conserved E3 ubiquitin ligase that regulates apoptosis, transcription, metabolism, development and DNA damage response via promoting ubiquitination and degradation of downstream targets [29]. UBR5 has been reported to be implicated in cancers such as lymphoma, ovarian, breast and gastric cancer [29,30]. Chung et al. found that UBR5-zinc finger protein 423 (ZNF423) fusion protein contributed to NPC cell transformation [31]. The Cancer Genome Atlas (TCGA) database shows increased UBR5 expression in NPC. However, its role in NPC is largely unknown. Besides, we predicted potential binding sites for HOXA9 in UBR5 using the JASPAR database. Although UBR5 and SIRT6 have not been linked, we found potential binding between UBR5 and SIRT6 through bioinformatics, suggesting that SIRT6 might be a ubiquitination substrate of UBR5.

In summary, we firstly demonstrate that the O-GlcNAcylation of HOXA9 promotes its stability and nuclear translocation, and subsequently HOXA9 controls ferroptosis by facilitating UBR5-dependent ubiquitination and degradation of SIRT6 to promote NPC progression. Our findings not only provide mechanistic insights into the pathogenesis of NPC, but also suggest HOXA9 as a prognostic biomarker and targeting ferroptosis as a therapeutic strategy for NPC.

Methods

Clinical specimens

Tumor tissues from NPC patients and normal nasopharyngeal tissues were collected at Hunan Cancer Hospital and The Affiliated Cancer Hospital of Xiangya School of Medicine, Central South University. Patients included in our study were $\geq$ 18-year-old, firstly diagnosed and did not receive any treatment. Patients with pregnancy, drug and alcohol abuse, other cancers are excluded. Patients provided written consent, and our study was approved by the Ethics Committee of Hunan Cancer Hospital.

Cell culture and treatment

NPC cell lines including 5-8F, NPC/HK1, HNE3 and C666-1 and nasopharyngeal epithelial NP69 cells were cultured in RPMI 1640 (Solarbio, Beijing, China) supplemented with 12 % fetal bovine serum (FBS, Cytiva, Marlborough, MA, USA). For inducing ferroptosis, cells were treated with erastin (Selleck Chemicals, Houston, TX, USA) at 0, 2.5, 5, 10, 20 or 40 μM or RSL3 (Selleck Chemicals) at 0.1, 0.5, 1, 5 or 10 μM for 24 hours in the presence or absence of ferrostatin-1 (Fer-1, Selleck Chemicals) at 5 μM. In some assays, cells were treated with cycloheximide (CHX, Selleck Chemicals) at 50 mg/mL for 0, 2, 4 or 8 hours or MG132 (Selleck Chemicals) at 10 μM for 4 hours. Cells were treated with Thiamet G (TMG, Selleck Chemicals) at 10 μM and OSMI-4 (Selleck Chemicals) at 20 μM for 24 h.

Cell transfection

For overexpression of HOXA9, UBR5 and SIRT6, the coding regions of HOXA9 and UBR5 were cloned into the pcDNA3.1 expression vector, respectively. Small hairpin RNAs against HOXA9 (sh-HOXA9#1 and sh-HOXA9#2), UBR5 (sh-UBR5#1 and sh-UBR5#2) and SIRT6 (sh-SIRT6) and negative control shRNAs (sh-NC) were provided by RiboBio (Guangzhou, China). NPC cells were transfected with various combinations of overexpressing constructs and shRNAs using Lipo 3000 reagent supplied by Thermo Fisher Scientific (Waltham, MA, USA) following the manual. Besides, sh-HOXA9, sh-UBR5 or sh-NC was inserted into the pGFP-C-shLenti lentiviral vector, and lentivirus was generated in HEK293T cells. Lentiviral supernatants were harvested for transducing NPC cells. FLAG-tagged HOXA9, FLAG-tagged HOXA9-T4A, FLAG-tagged HOXA9-S127A and MYC-tagged O-GlcNAc transferase (OGT) were transfected into HEK293T cells using Lipo 3000 reagent.

Cell Counting Kit-8 (CCK-8) assay

Cell viability was examined using CCK-8 assay. Briefly, cells were seeded and treated with erastin or RSL3 for 24 hours. Subsequently, medium was removed, and fresh medium (100 μL) was mixed with CCK-8 (10 μL, Beyotime, Shanghai, China) and added into each well. Cells were incubated for 2 hours, and the absorbance (450 nm) was measured.

Examination of ferroptosis hallmarks

NPC cells were lysed, and cell lysates were collected. Glutathione (GSH) and MDA were examined using Glutathione Colorimetric Detection Kit (Thermo Fisher Scientific) and malondialdehyde (MDA) Assay Kit (PromoCell, Heidelberg, Germany) following the manuals, respectively. In addition, Iron Assay Kit (Colorimetric) from Abcam (Cambridge, UK) was applied to detect the levels of total iron and Fe^{2+}. Iron reducer was added for total iron, and only buffer was added for Fe^{2+}.

Lipid peroxidation

For flow cytometry analysis of lipid peroxidation, cells were stained with BODIPY 581/591 C11 (Thermo Fisher Scientific) at 10 μM for half an hour at 37°C. After wash, cells were analyzed using the FITC channel.

Chromatin immunoprecipitation (ChIP)

NPC cells (~5 × 10^6) were incubated in 2 % formaldehyde solution for crosslink, and then lysed in lysis buffer supplemented with protease inhibitors. The lysates were collected and subjected to ultrasonication. Subsequently, DNA-protein fragments were harvested, and an HOXA9 antibody (5 μg, Proteintech, Rosemont, IL, USA) or normal rabbit IgG (5 μg, Proteintech) was added and incubated overnight. Next day, Protein A/G Magnetic Beads from Thermo Fisher Scientific were mixed with DNA-protein fragments and incubated for additional 2 hours with gentle rotation. Finally, DNA was eluted, and the enrichment of binding sites (site 1, 2 and 3) were determined by qPCR.

Dual-luciferase reporter assay

The promoter regions (promoter 1, 2 and 3) of UBR5 containing potential binding sites (site 1, 2 and 3) for HOXA9 were inserted into the Pgl3 vector (Promega, Madison, WI, USA). These reporters were transduced into NPC cells transfected with sh-NC, sh-HOXA9#1 or sh-HOXA9#2. After 48 hours, cells were harvested, and Dual-Glo Luciferase Assay System provided by Promega was used to examine luciferase activity.

Immunoprecipitation (IP) and ubiquitination and O-GlcNAcylation analysis

For analyzing the interaction between UBR5 and SIRT6, Co-IP assays were performed. In brief, NPC cells were lysed on ice, and cell lysates were centrifugated for collecting supernatants. An anti-SIRT6 antibody (2 μg, Abcam) or normal rabbit IgG (2 μg, Abcam) was mixed with the supernatants and incubated overnight. Next day, Protein A/G Magnetic Beads (Thermo Fisher Scientific) were added, mixed, and incubated for 2 hours with gentle rotation. Subsequently, proteins were recovered and applied for detecting the enrichment of UBR5 and SIRT6 by Western blotting. For determining the interaction between OGT and HOXA9, MYC-OGT and FLAG-HOXA9 were transfected into HEK293T cells, and cells were lysed. FLAG-HOXA9 was immuoprecipitated using Pierce Anti-DYKDDDDK Magnetic Agarose (Thermo Fisher Scientific), and the abundance of MYC-OGT and FLAG-HOXA9 was examined by Western blotting. For analyzing the ubiquitination of SIRT6, SIRT6 was immuoprecipitated with the anti-SIRT6 antibody from NPC cells transfected with empty vector or UBR5-overexpressing construct and subjected to western blotting for detecting the ubiquitination of SIRT6 using an anti-ubiquitin antibody (1:1000, Abcam). For analyzing the O-GlcNAcylation of HOXA9, HOXA9 was immuoprecipitated with the anti-HOXA9 antibody from NPC cells and subjected to Western blotting for detecting the O-GlcNAcylation of HOXA9 using an anti-RL2 antibody (1:1000, Abcam).

Immunofluorescence (IF) staining

After treatment, NPC/HK1 and C666-1 cells were washed and fixed in 4 % formaldehyde for 15 min. After wash, cells were permeabilized in 0.3 % Triton X-100 for 15 min and blocked in 10 % normal goat serum/PBS. Then, cells were incubated with an HOXA9 antibody (1:500, Invitrogen) overnight. Next day, cells were washed and incubated with AF594-conjugated goat-anti rabbit antibody (1:1000, Abcam) for 1 h. Cells were washed and mounted for imaging.

A subcutaneous NPC mouse model

BALB/c nude mice (male, 6-week-old, n = 24) were provided by Hunan Cancer Hospital and used for subcutaneous inoculation of NPC cells. Animal procedures complied with National Institutes of Health guidelines and approved by the Animal Care and Use Committee of Hunan Cancer Hospital. NPC cells (1 × 10^6) were stably transfected with sh-NC, sh-HOXA9 or sh-UBR5 through lentivirus and were subcutaneously injected into the right flanks. Erastin (10 mg/kg body weight) or vehicle was intraperitoneally administrated to mice every 72 hours for four weeks. Tumor volume was monitored using a caliper and calculated with the formula length × $\text{width}^2/2$. Finally, mice were sacrificed, and tumor were excised for imaging and weighted, which were used for subsequent immunohistochemical staining and Western blotting.

Immunohistochemical staining

Subcutaneous tumor tissues from mice were fixed, embedded in paraffin and sliced into 5-μm sections. Sections were deparaffinized, dehydrated and subjected into antigen retrieval. Subsequently, sections were blocked and incubated with an anti-HOXA9 (1:50, Abcam), anti-Ki-67 (1:100, Abcam) or anti-GPX4 (1:50, Abcam) overnight. Next day, sections were rinsed and incubated with a horseradish peroxidase (HRP)-conjugated goat-anti rabbit antibody for 1 hour. 3,3'-Diaminobenzidine (DAB, Beyotime) was used to visualize signals.

qRT-PCR

Total RNA was extracted from tumor tissues and NPC cells using Trizol reagent (Thermo Fisher Scientific). RNA was reversely transcribed into cDNA with High-Capacity cDNA Reverse Transcription Kit (Thermo Fisher Scientific). HOXA9, UBR5 and SIRT6 were examined by quantitative PCR with SYBR Green (Beyotime) and normalized to GAPDH using the $2^{-\Delta\Delta Ct}$ method. Primers were listed in Table 1.

Western blotting

Protein was extracted from tumor tissues and NPC cells and quantified using BCA kit from Thermo Fisher Scientific. 30 μg of protein was electrophoresed and transferred to polyvinylidene fluoride (PVDF) membrane (Bio-Rad, Hercules, CA, USA). Subsequently, membranes were blocked and incubated with an anti-HOXA9 (1:1000), anti-ACSL4 (1:1000), anti-GPX4 (1:500), anti-SIRT6 (1:1000), anti-UBR5 (1:500), anti-NCOA4 (1:1000), anti-FTH1 (1:1000), and anti-GAPDH (1:5000) overnight. Next day, membranes were washed and incubated with an HRP-conjugated goat-anti rabbit secondary antibody for 1 hour. Finally, bands were visualized by enhanced chemiluminescence (ECL) substrate (Bio-Rad). Band intensity was analyzed with the ImageJ software.

Statistical analysis

Data were presented as mean ± standard deviation. The variance of two and more groups were analyzed using the Student's test and one-way analysis of variance (ANOVA), respectively. $p < 0.05$ was

Table 1
qRT-PCR primers.

Genes	Primer sequences (5′-3′)
HOXA9	Forward: 5'-CCACGCTTGACACTCACACT-3' Reverse: 5'-TCGTCTTTTGCTCGGTCTTT-3'
UBR5	Forward: 5'-GACGCGAGAACTCTTGGAAC-3' Reverse: 5'-TTCAAATGGATTTGGGGGTA-3'
SIRT6	Forward: 5'-AGGATGTCGGTGAATTACGC-3' Reverse: 5'-CCAGTTCCCACACCTTCC-3'
GAPDH	Forward: 5'-GGATTTGGTCGTATTGGG-3' Reverse: 5'-GGAAGATGGTGATGGGATT-3'

statistically significant. *p <0.05, **p <0.01 and ***p <0.001.

Results

The expression of HOXA9 was increased in NPC

To analyze potential regulators of NPC progression, we identified top 10 genes with significant up- and down-regulation including upregulated TMEM68, SUOX, SLC20A2, RAC1, NFE2L2, HOXA9, FBXO32, FAM110A, DNAJB6 and BAHCC1 and downregulated TBL1XR1, SETBP1, PLEKHG2, GPD1L, FNBP1, EIF1B, CNPY3, CA8, C21orf7 and ATM through the GEO dataset (GSE68799, NPC n = 42; Normal nasopharyngeal tissue n = 4.) analysis (Fig. 1A). Subsequently, we determined the expression of the upregulated genes in nasopharyngeal epithelial cell NP69 and NPC cell lines 5-8F, NPC/HK1, HNE3, and C666-1, and HOXA9 showed the most significant change among them (Fig. 1B). Thus, we decided to focus the roles of HOXA9 in this study. Through the GEO database (GSE68799) analysis, we found that HOXA9 expression was significantly increased in NPC (Fig. 1C). IHC results also indicated that HOXA9 was increased in tumor tissues of NPC patients (Fig. 1D). High protein and mRNA levels of HOXA9 were observed in NPC cell lines 5-8F, NPC/HK1, HNE3, and C666-1 compared to nasopharyngeal epithelial cell NP69 (Fig. 1E and F). These observations suggested that HOXA9 might accelerate NPC progression.

Knockdown of HOXA9 enhanced ferroptosis in NPC cells

A recent study has reported the implication of HOXA9 in ferroptosis in acute myeloid leukemia [32], we determined to explore whether HOXA9 regulates NPC progression by modulating ferroptosis. HOXA9 was knocked down through shRNA transfection, which was confirmed by qRT-PCR and Western blotting (Supplementary Fig. 1A and B). Subsequently, C666-1 and NPC/HK1 cells were treated with various concentrations of erastin or RSL3, wildly used ferroptosis inducers. We

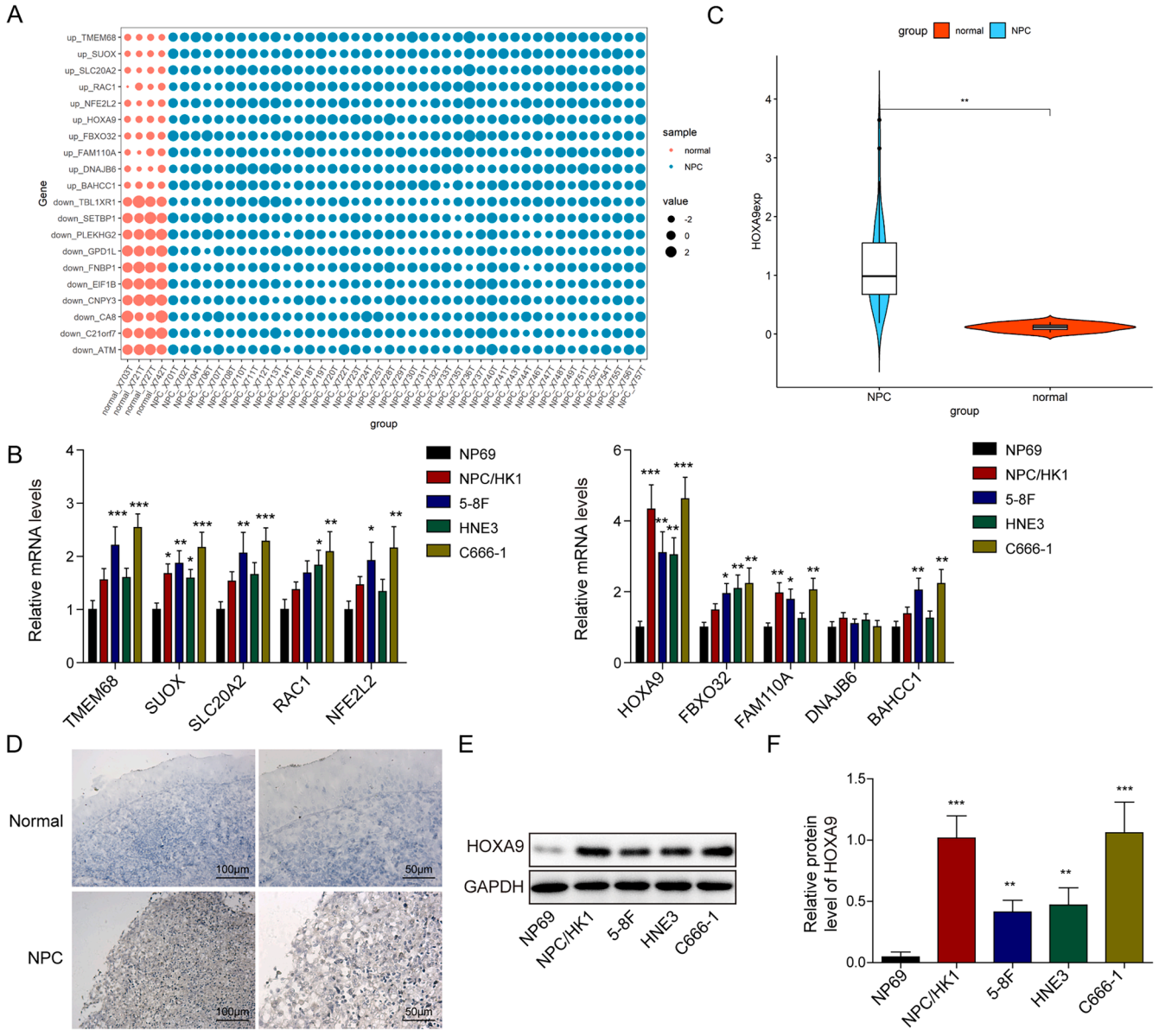

Fig. 1. The expression of HOXA9 was increased in NPC. (A) GEO dataset (GSE68799) analysis of differentially expressed genes in NPC (normal, n = 4; NPC, n = 42). (B) qRT-PCR analysis of TMEM68, SUOX, SLC20A2, RAC1, NFE2L2, HOXA9, FBXO32, FAM110A, DNAJB6 and BAHCC1 in NP69, 5-8F, NPC/HK1, HNE3 and C666-1 cells. (C) GEO database (GSE68799) analysi of HOXA9 expression in NPC. (D) IHC detected HOXA9 level in tumor tissues of patients. (Scale bar, 100 and 50 μm). Western blotting (E) and qRT-PCR (F) analysis of HOXA9 in NP69, 5-8F, NPC/HK1, HNE3 and C666-1 cells. * p < 0.05, ** p < 0.01 and *** p < 0.001.

found that the low viability of erastin or RSL3-treated NPC cells was further enhanced by HOXA9 knockdown, but this effect was reversed by the treatment of the ferroptosis inhibitor Fer-1 (Fig. 2A). Additionally, the inhibition in NPC cell viability by HOXA9 silencing was weakened by ferroptosis inhibitor Fer-1, but not significantly affected by apoptosis inhibitor (ZVAD-FMK), necrosis inhibitor (Nec-1) or autophagy inhibitor (3-MA) (Supplementary Fig. 2), suggesting the involvement of HOXA9 in ferroptosis. Moreover, HOXA9 knockdown elevated levels of MDA, a final product of lipid peroxidation, total iron and Fe^{2+}, and erastin or RSL3-induced MDA, total iron and Fe^{2+} were further enhanced by knockdown of HOXA9 in C666-1 and NPC/HK1 cells (Fig. 2B-D). Besides, HOXA9 knockdown inhibited GSH, and the level of GSH was reduced by erastin or RSL3 treatment, which was further suppressed by HOXA9 knockdown in NPC cells (Fig. 2E). Knockdown of HOXA9 enhanced lipid peroxidation and augmented erastin or RSL3-induced lipid peroxidation (Fig. 2F and G). Furthermore, we examined the expression of SIRT6 and ferroptosis-related markers including ACSL4 and GPX4. We found that knockdown of HOXA9 enhanced the expression of ACSL4 and SIRT6 but reduced GPX4 expression in erastin or RSL3-treated C666-1 and NPC/HK1 cells (Fig. 2H and I). Collectively, these results indicated that knockdown of HOXA9 strengthened ferroptosis in NPC cells.

O-GlcNAcylation stabilized HOXA9 and facilitated its nuclear translocation in NPC cells

O-GlcNAcylation is one of the post-translational modifications of proteins that may play an important role in protein stability [33]. O-GlcNAcylation is abnormally upregulated in most cancers, promoting cancer progression [34], but its role in NPC has never been reported. Also, recent studies has revealed that the regulatory function of O-GlcNAcylation in ferroptosis [35]. Intriguingly, we identified potential O-GlcNAc sites in HOXA9 through YinOYang-1.2 (https://services.healthtech.dtu.dk/services/YinOYang-1.2/) analysis (Fig. 3A). Thus, HOXA9 was immunoprecipitated, and its O-GlcNAcylation was determined with Western blotting. We observed increased O-GlcNAcylation of HOXA9 in NPC cells compared to NP69 cells (Fig. 3B). Then, we treated NPC/HK1 and C666-1 cells with TMG, a O-GlcNAcase (OGA) inhibitor, or OSMI-4, O-GlcNAc transferase (OGT) inhibitor. The level of O-GlcNAc has been reported to be increased by TMG but decreased by OSMI-4 [36,37]. HOXA9 level was increased in TMG-treated cells but decreased in OSMI-4-treated cells (Fig. 3C). MYC-tagged OGT and FLAG-tagged HOXA9 were co-expressed in HEK293T cells, and MYC-OGT could be co-immunoprecipitated by FLAG-HOXA9 (Fig. 3D). Subsequently, the threonine at Position 4 (T4) and serine at Position 127 (S127) of human HOXA9 were mutated to alanine (A) and transfected into HEK293T cells. The level of O-GlcNAc was largely eliminated by S127A, but it was not affected by T4A (Fig. 3E), suggesting that the S127 was the O-GlcNAc site of HOXA9, and the serine was highly conservative among various species (Fig. 3F). To determine whether O-GlcNAcylation affects HOXA9 stability, MYC-tagged OGT and FLAG-tagged HOXA9 were transfected into HEK293T cells and treated with CHX. The degradation of HOXA9 was significantly slowed down by MYC-tagged OGT co-expression (Fig. 3G). However, the degradation of the mutated HOXA9 (S127A) was not affected by MYC-tagged OGT co-expression (Fig. 3G). Furthermore, we found that the nuclear translocation of HOXA9 was significantly enhanced by TMG but reduced by OSMI-4 in NPC/HK1 and C666-1 cells (Fig. 3H). Thus, these results suggested that O-GlcNAcylation stabilized HOXA9 and facilitated its nuclear translocation in NPC cells.

HOXA9 directly bound to the promoter of UBR5 to promote its expression in NPC cells

Cai et al. found that SIRT6 silencing downregulated GPX4 and promoted ferroptosis in gastric cancer cells [25]. However, Gong et al. founded that SIRT6 increased the level of ROS, promoted ferroptosis and repressed glycolysis by blocking the activation of the NF-κB pathway in pancreatic cancer [38]. The above contents suggest that SIRT6 can be involved in the regulation of ferroptosis in tumor cells, and its effect on iron death is different in different tumors. Therefore, we further explored the role of SIRT6 on ferroptosis in NPC. To determine the mechanism by which HOXA9 regulates ferroptosis and SIRT6 expression, we examined the mRNA level of SIRT6 in NPC/HK1 and C666-1 cells transfected with sh-NC, sh-HOXA9#1 or sh-HOXA9#2, but no significant change was observed (Fig. 4A). However, BioGRID database analysis revealed multiple post-translational ubiquitination modification sites in SIRT6 (Fig. 4B). We hypothesized that HOXA9 might regulate the ubiquitination modification of SIRT6 through ubiquitin ligase. Thus, we analyzed the expression of various ubiquitin ligases in HOXA9-knockdown cells and found that UBR5 showed the most significant downregulation (Fig. 4C). Moreover, we found that UBR5 expression was increased in head and neck squamous cell carcinoma by GEPIA2 database (http://gepia2.cancer-pku.cn/#index) (Fig. 4D). In addition, we found that UBR5 was highly expressed in 5-8F, NPC/HK1, HNE3 and C666-1 cells (Fig. 4E-G). Intriguingly, both mRNA and protein levels of UBR5 were significantly suppressed by HOXA9 knockdown in C666-1 and NPC/HK1 cells (Fig. 4H-J). These data implied that HOXA9 positively regulated UBR5 expression in NPC cells. To investigate how HOXA9 regulates UBR5 expression, three potential binding sites for HOXA9 in the promoter region of UBR5 were predicted using the JASPAR database (Fig. 4K). Furthermore, ChIP assays showed that the Site 1, not Site2 and 3, could be efficiently immunoprecipitated by anti-HOXA9 (Fig. 4L). Additionally, the luciferase activity of the UBR5 Pro1 (unmutated Site1 and mutated Site2 and 3) reporter was obviously reduced by HOXA9 knockdown, and the luciferase activity of the Pro2 (unmutated Site2 and mutated Site1 and 3) and 3 (unmutated Site3 and mutated Site1 and 2) reporters were unaffected (Fig. 4M). Our findings demonstrated that HOXA9 directly bound to the promoter of UBR5 to regulate its expression in NPC cells.

UBR5 facilitated the ubiquitination and degradation of SIRT6 to reduce its expression in NPC cells

To further explore downstream targets of UBR5, UBR5 was overexpressed through UBR5-overexpressing vector transfection in C666-1 and NPC/HK1 cells, which was confirmed by qRT-PCR and Western blotting (Fig. 5A and B). Intriguingly, we observed that UBR5 overexpression markedly inhibited SIRT6 expression, but UBR5-mediated suppression was reversed by MG132 treatment (Fig. 5C), suggesting that UBR5 might regulate SIRT6 degradation. Furthermore, Co-IP assays showed that UBR5 was co-immunoprecipitated by the SIRT6 antibody (Fig. 5D), suggesting the interaction between SIRT6 and UBR5. Besides, we found that overexpression of UBR5 dramatically enhance SIRT6 ubiquitination in C666-1 and NPC/HK1 cells (Fig. 5E). Subsequently, NPC cells were treated with CHX for inhibition of protein synthesis, and the protein levels of UBR5 and SIRT6 were examined. With increasing incubation time, the level of SIRT6 was gradually reduced, and overexpression of UBR5 significantly enhanced SIRT6 degradation and reduced the half-time of SIRT6 in NPC cells (Fig. 5F). To conclude, UBR5 reduced SIRT6 expression via promoting its ubiquitination and degradation in NPC cells.

O-GlcNAc-modified HOXA9 inhibited ferroptosis via targeting UBR5 in NPC cells

HOXA9 was overexpressed in C666-1 and NPC/HK1 cells through HOXA9-overexpressing vector transfection (Supplementary Fig. 1C and D), and UBR5 was knocked down through shRNA transfection (Supplementary Fig. 1E and F). NPC cells were treated with OSMI-4 for reducing O-GlcNAcylation and erastin for inducing ferroptosis. OSMI-4 impaired the viability of C666-1 and NPC/HK1 cells in the presence or

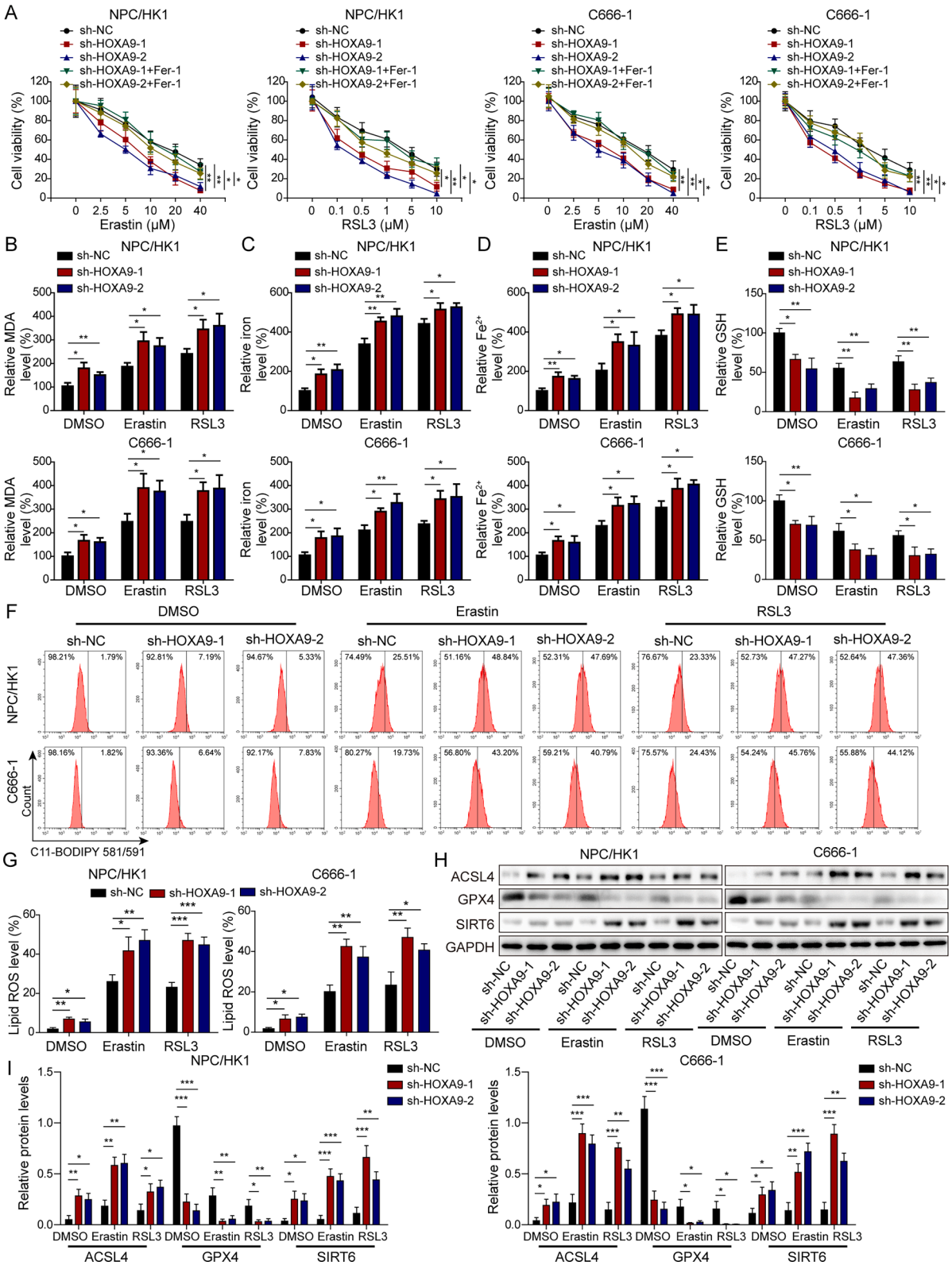

Fig. 2. Knockdown of HOXA9 enhanced ferroptosis in NPC cells. NPC/HK1 and C666-1 cells were transfected with sh-NC, sh-HOXA9#1 or sh-HOXA9#2 and treated with Erastin at 0, 2.5, 5, 10, 20 or 40 μM or RSL3 at 0.1, 0.5, 1, 5 or 10 μM for 24 hours in the presence or absence of Fer-1 at 5 μM. DMSO was used as the solvent control. qRT-PCR (A) Cell viability was evaluated with CCK-8 after treatment with different concentrations of Erastin and RSL3. Relative MDA (B), total iron (C), Fe^{2+} (D), and GSH (E) in NPC/HK1 and C666-1 cells after Erastin (10 μM) or RSL3 (1 μM) treatment. (F and G) Measurement of lipid peroxidation by flow cytometry after Erastin (10 μM) or RSL3 (1 μM) treatment. (H and I) Western blotting analysis of ACSL4, GPX4, SIRT6 and GAPDH after Erastin (10 μM) or RSL3 (1 μM) treatment. * $p < 0.05$, ** $p < 0.01$ and *** $p < 0.001$.

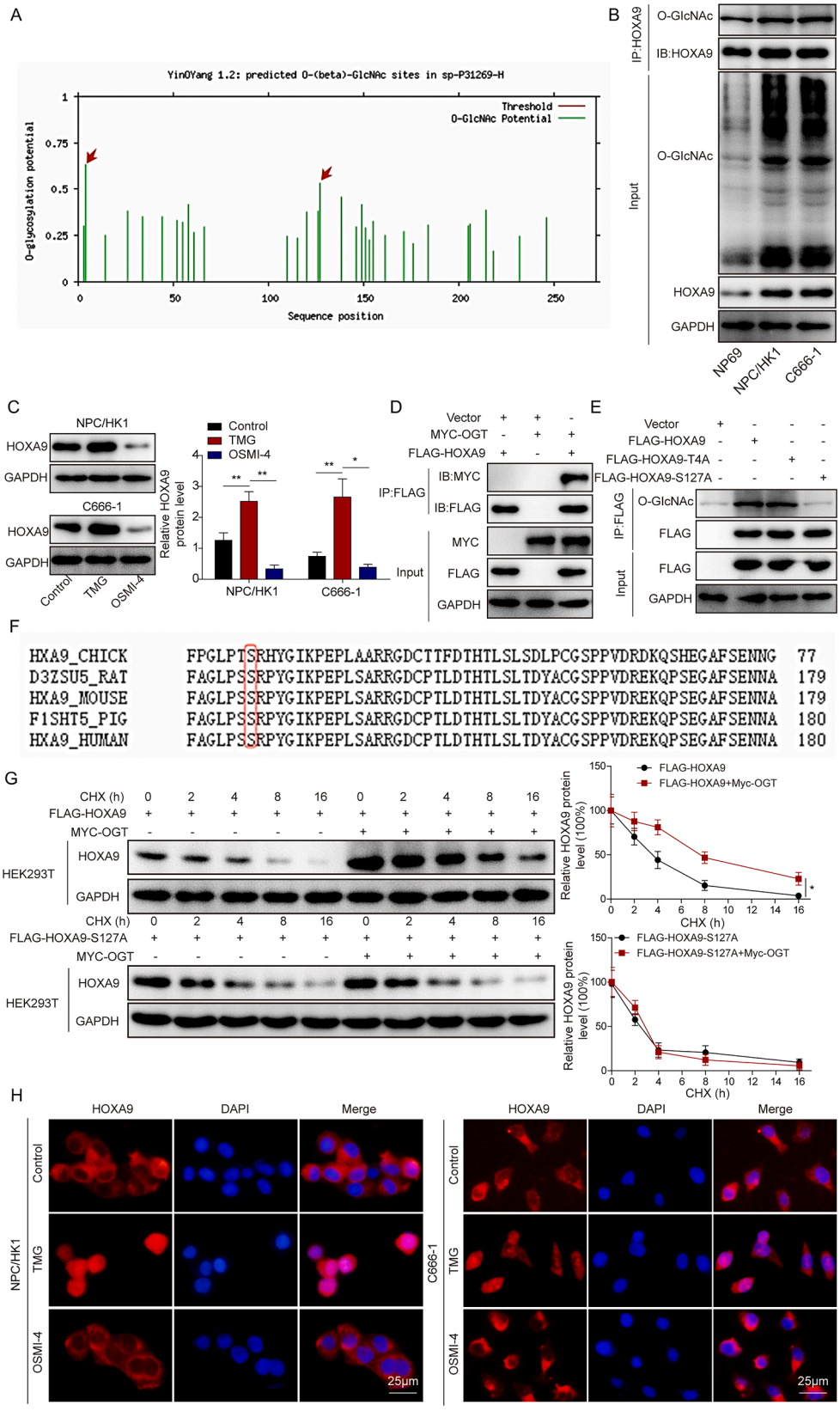

(caption on next page)

Fig. 3. O-GlcNAcylation stabilized HOXA9 and facilitated its nuclear translocation in NPC cells. (A) Two potential O-GlcNAc modification sites (Thr4 and Ser127) on HOXA9 was predicated through YinOYang-1.2. (B) HOXA9 was immunoprecipitated, and its O-GlcNAcylation was examined by Western blotting in NP69, NPC/HK1 and C666-1 cells. (C) Western blotting analysis of HOXA9 and GAPDH in NPC/HK1 and C666-1 cells treated with control, TMG and OSMI-4. (D) MYC-OGT and FLAG-HOXA9 were transfected into HEK293T cells, and FLAG-HOXA9 was immunoprecipitated. The abundance of MYC-OGT and FLAG-HOXA9 was determined with Western blotting. (E) HEK293T cells were transfected with FLAG-HOXA9, FLAG-HOXA9-T4A or FLAG-HOXA9-S127A. FLAG was immunoprecipitated, and its O-GlcNAcylation was examined by Western blotting. (F) Homology analysis of HOXA9 in different species. (G) Protein levels of HOXA9 in cells transfected with MYC-OGT, FLAG-HOXA9 or FLAG-S127A and treated with CHX for 0, 2, 4, 8 or 16 hours. (H) IF staining of HOXA9 in NPC/HK1 and C666-1 cells treated with control, TMG and OSMI-4. Scale bar, 25 μm * $p < 0.05$, ** $p < 0.01$ and *** $p < 0.001$.

absence of erastin, but it was improved by HOXA9 overexpression, and the protective effect was abolished by simultaneous UBR5 knockdown (Fig. 6A). In addition, increased levels of MDA, total iron and Fe^{2+} in OSMI-4-treated cells were inhibited by HOXA9 overexpression, which was abrogated by UBR5 knockdown in the presence or absence of erastin (Fig. 6B-D). The level of GSH was reduced by OSMI-4 treatment and restored by HOXA9 overexpression, which was reversed by UBR5 knockdown (Fig. 6E). Furthermore, increased lipid ROS in OSMI-4-treated NPC cells in the presence or absence of erastin was reduced by HOXA9 overexpression, but it was counteracted by UBR5 knockdown (Fig. 6F and G). OSMI-4 treatment promoted the expression of ACSL4 and SIRT6 and suppressed the expression of UBR5 and GPX4 in NPC cells, but their expression patterns were reversed by overexpression of HOXA9, which was abrogated by UBR5 knockdown (Fig. 6H and I). These results indicated that O-GlcNAc-modified HOXA9 inhibited ferroptosis in NPC cells dependent on UBR5.

UBR5 suppressed ferroptosis through SIRT6 in NPC cells

Subsequently, UBR5 and SIRT6 were knockdown in C666-1 and NPC/HK1 cells, and SIRT6 knockdown efficiency was confirmed by qRT-PCR and Western blotting (Supplementary Fig. 1G and H). Knockdown of UBR5 reduced cell viability, and erastin-induced reduction in cell viability was further enhanced by UBR5 knockdown, but these effects were abolished by SIRT6 knockdown (Fig. 7A). Moreover, UBR5 knockdown elevated the levels of MDA, total iron and Fe^{2+} and reduced GSH level in NPC cells, which were all reversed by simultaneous SIRT6 knockdown in the presence or absence of erastin (Fig. 7B-E). Knockdown of UBR5-induced lipid ROS was suppressed by SIRT6 knockdown (Fig. 7F and G). ACSL4 and SIRT6 were upregulated, and GPX4 was downregulated by UBR5 knockdown in DMSO or erastin-treated NPC cells, and their expression patterns were reversed by simultaneous SIRT6 knockdown (Fig. 7H and I). To examine the involvement of NCOA4 and FTH1, we examined their expression. UBR5 knockdown enhanced NCOA4 expression but reduced FTH1 expression, and their expression was reversed by SIRT6 knockdown (Fig. 7H and I), suggesting the involvement of the SIRT6/NCOA4/FTH1 axis. Taken together, our findings implied that UBR5-mediated suppression of ferroptosis was dependent on inhibition of SIRT6 in NPC cells.

Knockdown of HOXA9 or UBR5 promoted ferroptosis through SIRT6 and repressed NPC growth in mice

A subcutaneous NPC mouse model was established to explore whether knockdown of HOXA9 or UBR5 regulates tumor growth *in vivo*. Tumor size, volume and weight were reduced by erastin administration (Fig. 8A-C). Intriguingly, knockdown of HOXA9 or UBR5 further reduced tumor size, volume, and weight, suggesting that erastin-mediated anti-tumor activity was further strengthened by HOXA9 or UBR5 knockdown (Fig. 8A-C). The expression of UBR5 were decreased, and SIRT6 was upregulated in tumor tissues from erastin-treated mice (Fig. 8D). Knockdown of HOXA9 or UBR5 further enhanced SIRT6 expression (Fig. 8D and E). Additionally, erastin raised the expression of ACSL4 and inhibited GPX4 expression in tumor tissues, and simultaneous knockdown of HOXA9 or UBR5 further promoted the expression of ACSL4 and reduced GPX4 expression (Fig. 8F and G), demonstrating that knockdown of HOXA9 or UBR5 enhanced erastin-induced ferroptosis. Similarly, IHC staining showed that the expression of GPX4 and Ki-67, a cell proliferation marker, was inhibited by erastin and further reduced by simultaneous knockdown of HOXA9 or UBR5 (Fig. 8H), suggesting that knockdown of HOXA9 or UBR5 inhibited NPC cell proliferation. Collectively, these data suggested that knockdown of HOXA9 or UBR5 enhanced ferroptosis via SIRT6 and inhibited NPC growth *in vivo*.

Discussion

NPC is the most frequent head and neck cancer in Southern China, causing serious health and economic burden [1,39]. Epstein-Barr virus infection, genetic and environmental factors may contribute to its distinct geographical prevalence [40,41]. Due to its inconspicuous symptoms and concealed localization, many NPC patients are not diagnosed and treated timely, leading to increased mortality [42]. Distant metastasis is also a major challenge for NPC treatment [43]. Novel therapeutic targets need to be discovered for improving advanced NPC treatment. In our study, we reported increased HOXA9 expression in NPC patients. Further investigations demonstrated that O-GlcNAcylation improved HOXA9 stability and enhanced its nuclear translocation, and HOXA9 reduced ferroptosis via promoting UBR5 expression and subsequent SIRT6 degradation in NPC cells. Intriguingly, silencing of HOXA9 or UBR5 facilitated ferroptosis and reduced NPC growth *in vivo*.

Ferroptosis can function as a double-edged sword inhibiting or accelerating the progression of various cancers, which has been developed as a promising target for cancer treatment [44,45]. Ferroptosis shows several hallmarks such as iron accumulation, increased lipid peroxidation, impaired antioxidant defense and decreased GPX4 expression [46]. Increasingly, ferroptosis is being targeted for providing new opportunities for cancer treatment including NPC. The sensitivity of NPC cells to radiotherapy can be improved by targeting ferroptosis [11]. Yuan et al. found that Epstein–Barr virus (EBV) infection-induced GPX4 to repress ferroptosis of NPC cells and tumor cell proliferation [47]. In consistence, we observed that triggering ferroptosis by combined gene manipulation and erastin greatly suppressed NPC growth in mice. Therefore, ferroptosis inducers, such as small molecules, may contribute to suppressing chemoresistance and NPC progression and developed as combined therapeutic strategies with other anti-tumor drugs. RSL3, a ferroptosis inducer, has been reported to fail to deplete GSH [27]. However, growing evidence has shown that RSL3 can reduce GSH level as we report in this study [48,49]. The regulatory mechanism is still unknown, but the action mode of RSL3 may be different in diverse cells due to various cellular microenvironment. In cardiomyocytes, isolated mitochondrial shows high sensitivity of GSH to RSL3, and GSH level is significantly decreased after RSL3 treatment [49]. In addition, a recent study suggests that RSL3 is not a direct inhibitor of GPX4 but of TXNRD1 [50], and TXNRD1 has been reported to facilitate the synthesis of GSH [51], suggesting that RSL3 may reduce GSH level through inhibiting TXNRD1.

HOXA9 plays important roles in regulating the progression of various cancers [52,53]. To the best of our knowledge, only one study reported that HOXA9 was upregulated in NPC and its increased expression was associated with poor prognosis [19]. However, the regulatory mechanism by which HOXA9 regulates NPC progression has not been reported yet. Reduced HOXA9 expression was reported to enhance cell death in

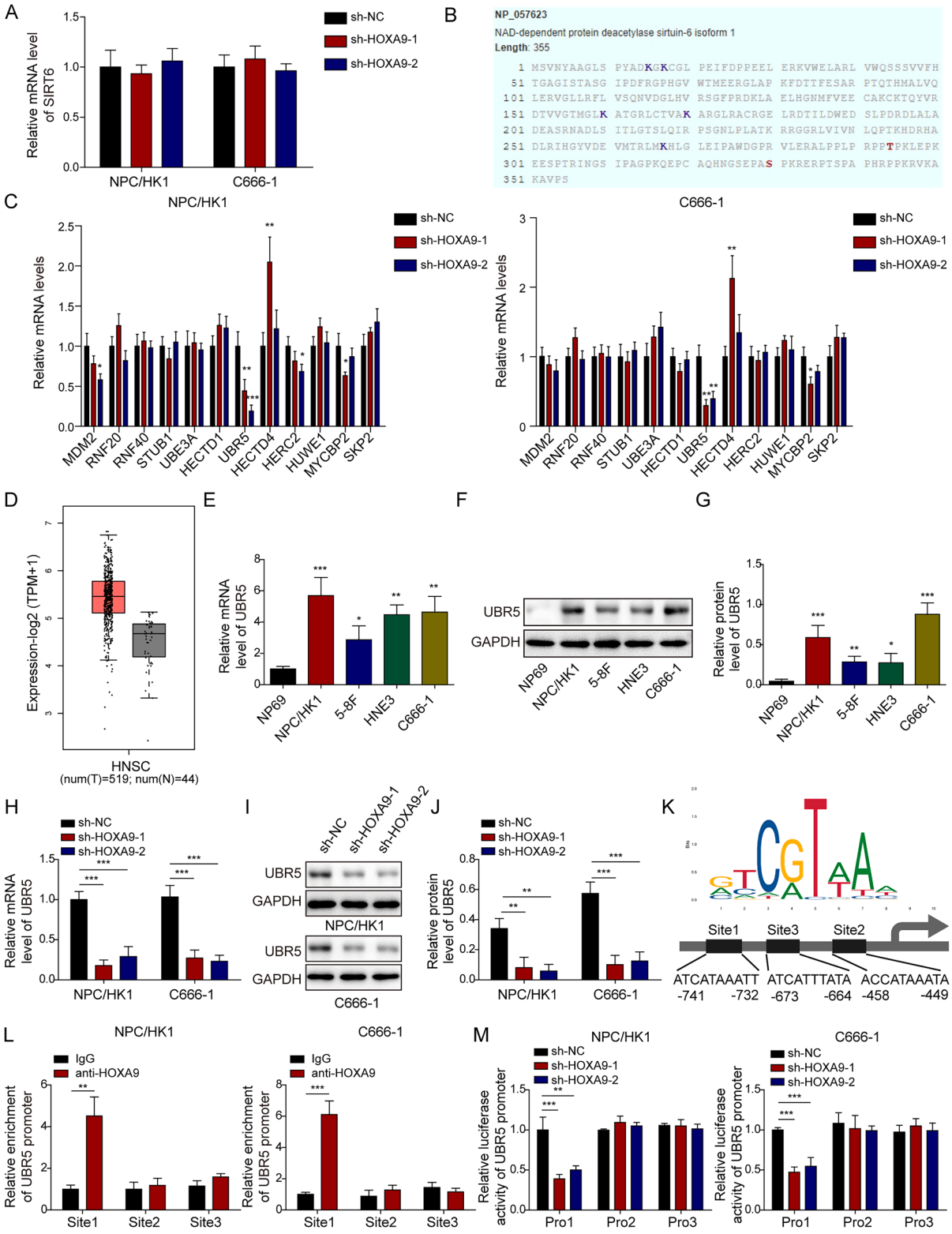

Fig. 4. HOXA9 directly bound to the promoter of UBR5 to promote its expression in NPC cells. (A) qRT-PCR analysis of SIRT6 in NPC/HK1 and C666-1 cells transfected with sh-NC, sh-HOXA9#1 or sh-HOXA9#2. (B) Multiple potential ubiquitination modification sites in SIRT6 was predicted through BioGRID database analysis. (C) qRT-PCR analysis of MDM2, RNF20, RNF40, STUB1, UBE3A, HECTD1, UBR5, HECTD4, HERC2, HUWE1, MYCBP2 and SKP2 in NPC/HK1 and C666-1 cells transfected with sh-NC, sh-HOXA9#1 or sh-HOXA9#2. (D) GEPIA2 database analysis of UBR5 expression in head and neck squamous cell carcinoma. qRT-PCR (E) and Western blotting (F and G) analysis of UBR5 in NP69, 5-8F, NPC/HK1, HNE3 and C666-1 cells. qRT-PCR (H) and Western blotting (I and J) analysis of UBR5 in NPC/HK1 and C666-1 cells transfected with sh-NC, sh-HOXA9#1 or sh-HOXA9#2. (K) Prediction of three binding sites for HOXA9 in the promoter of UBR5 through JASPAR. (L) The binding site for HOXA9 in the promoter of UBR5 was determined by ChIP assays. (M) The luciferase activity of UBR5 reporters in NPC/HK1 and C666-1 cells transfected with sh-NC, sh-HOXA9#1 or sh-HOXA9#2. * $p < 0.05$, ** $p < 0.01$ and *** $p < 0.001$.

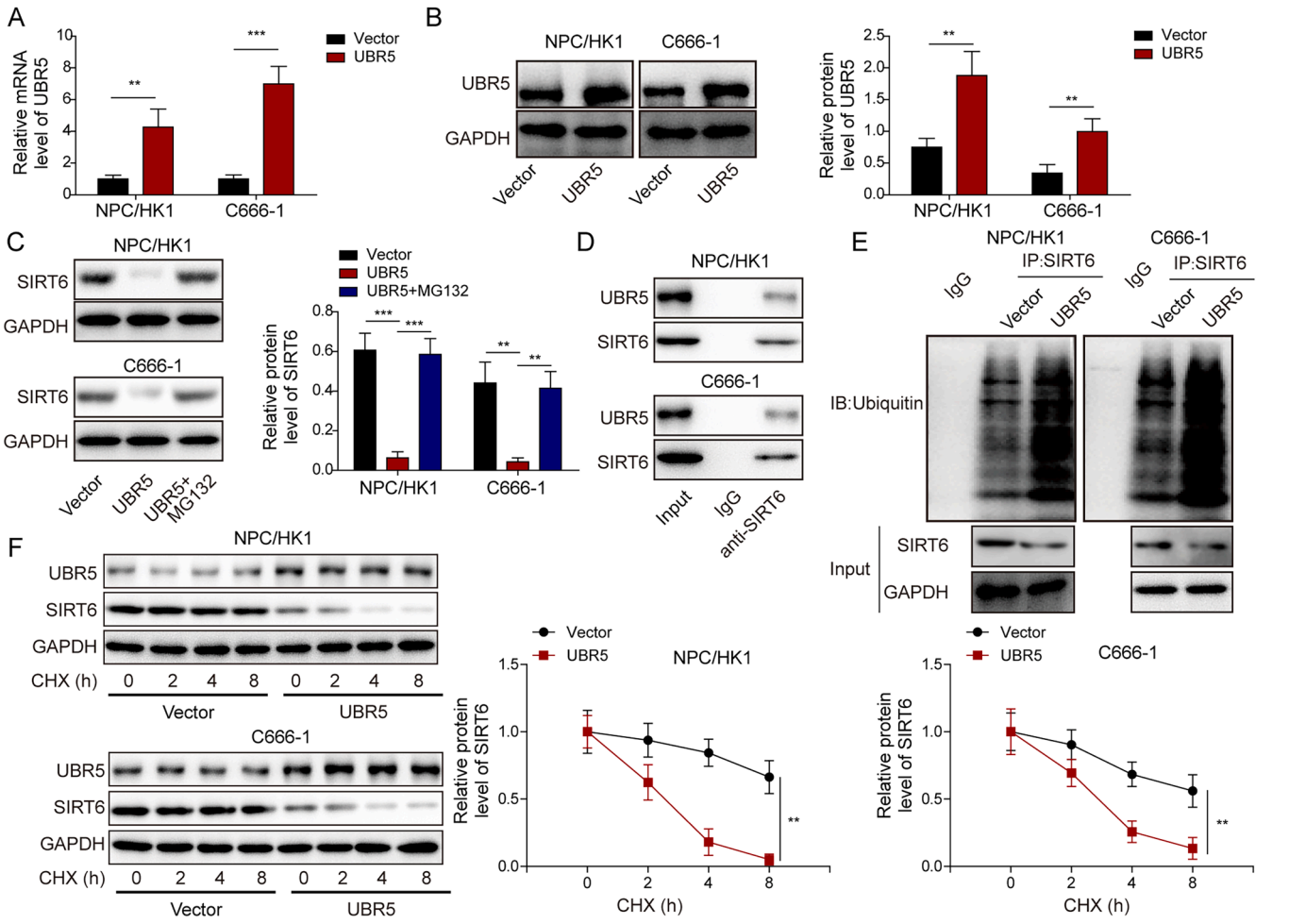

Fig. 5. UBR5 facilitated the ubiquitination and degradation of SIRT6 to reduce its expression in NPC cells. qRT-PCR (A) and Western blotting (B) analysis of UBR5 in NPC/HK1 and C666-1 cells transfected with empty vector or UBR5-overexpressing vector. (C) Protein levels of SIRT6 in cells transfected with empty vector or UBR5-overexpressing vector and UBR5-overexpressing cells treated with MG132. (D) Co-IP assays were applied to evaluate the interaction between UBR5 and SIRT6. (E) SIRT6 ubiquitination analysis in cells transfected with empty vector or UBR5-overexpressing vector. (F) Protein levels of UBR5 and SIRT6 in cells transfected with empty vector or UBR5-overexpressing vector and treated with CHX for 0, 2, 4 or 8 hours. * $p < 0.05$, ** $p < 0.01$ and *** $p < 0.001$.

leukemia [54]. Ferroptosis is an iron-dependent cell death, but no report has directly linked HOXA9 to ferroptosis to our knowledge. Importantly, we found that knockdown of HOXA9 promoted ferroptosis in NPC, identifying a novel regulator of ferroptosis in NPC.

O-GlcNAcylation regulates protein–protein interaction, protein stability and subcellular localization [55]. Song et al. found that DOT1L O-GlcNAcylation promoted its protein stability [56]. O-GlcNAcylation of nuclear factor kappa B (NF-κB) promotes its nuclear translocation [57]. However, no evidence has linked O-GlcNAcylation to HOXA9. We found that the O-GlcNAc site of HOXA9 was S127, and O-GlcNAcylation could maintain HOXA9 stability and facilitated its nuclear translocation in NPC. In addition, the important roles of O-GlcNAcylation in ferroptosis attract much attention in recent years [35]. O-GlcNAcylation senses the ferroptotic stress and coordinates ferritinophagy and mitophagy to activate ferroptosis [22]. In liver cancer, O-GlcNAcylation promotes sensitivity to RSL3-induced ferroptosis through the YAP/TFRC pathway [58]. However, no direct evidence linking O-GlcNAcylation, ferroptosis and NPC progression. Here, we reported that O-GlcNAcylation-mediated increased stability and nuclear translocation of HOXA9 suppressed ferroptosis in NPC, revealing a novel mechanism underlying ferroptosis regulation in NPC.

As a homeodomain-containing transcription factor, HOXA9 regulates the expression of downstream targets, such as CDX4, IGF1 and RUNX2 [59,60]. Here, we identified UBR5 as a novel target of HOXA9, and HOXA9 directly bound to the promoter of UBR5 to enhance its transcription in NPC cells. UBR5, a E3 ubiquitin-protein ligase that modulates protein levels through mediating ubiquitination and degradation [61], is becoming a vital regulator in various cancers [29,62]. Li and colleagues reported that UBR5 enhanced the metastasis of pancreatic carcinoma by promoting CAPZA1 degradation [63]. UBR5-mediated ubiquitination and degradation of targets are implicated in various cellular processes including cell cycle and DNA damage [64,65]. However, the roles of UBR5 in ferroptosis and NPC are unknown. We found that knockdown of UBR5 enhanced ferroptosis in NPC cells, and HOXA9-mediated regulation of ferroptosis was dependent on UBR5 for the first time. Importantly, combined UBR5 knockdown and erastin markedly promoted ferroptosis and restrained NPC growth in mice. Our findings demonstrated a novel role of UBR5 in regulating ferroptosis.

Sirtuin 6 (SIRT6) belongs to class III histone deacetylase family and plays key roles in DNA damage repair, anti-aging, chromatin regulation and tumor suppression [23]. SIRT6 was reported to be downregulated in NPC cell lines and tissues, and its overexpression enhanced NPC cell apoptosis [24]. Silencing of SIRT6 enhanced the accumulation of reactive oxygen species (ROS), MDA and Fe^{2+} and improved sorafenib chemosensitivity of gastric cancer cells via promoting ferroptosis [25]. Although UBR5 and SIRT6 have not been linked, we found potential binding between UBR5 and SIRT6 via analyzing the BioGRID database.

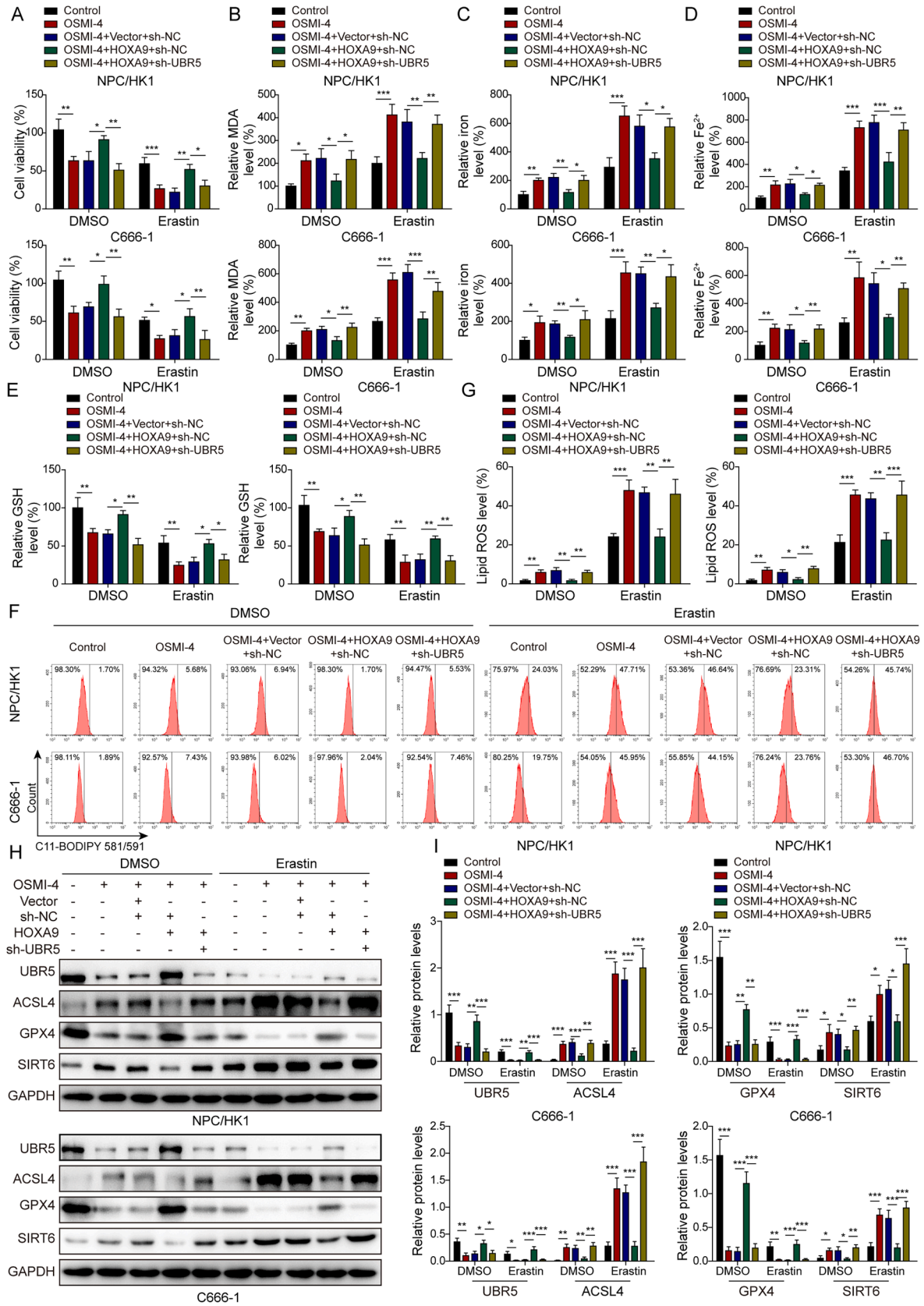

Fig. 6. O-GlcNAc-modified HOXA9 inhibited ferroptosis via targeting UBR5 in NPC cells. NPC/HK1 and C666-1 cells were transfected with Vector + sh-NC, HOXA9 + sh-NC or HOXA9 + sh-UBR5 and treated with Erastin at 10 μM and OSMI-4 at 20 μM for 24 hours. DMSO was used as the solvent control. (A) Cell viability was evaluated with CCK-8. Relative MDA (B), total iron (C), Fe^{2+} (D), and GSH (E) in NPC/HK1 and C666-1 cells. (F and G) Measurement of lipid peroxidation. (H and I) Western blotting analysis of UBR5, ACSL4, GPX4, SIRT6 and GAPDH. * $p < 0.05$, ** $p < 0.01$ and *** $p < 0.001$.

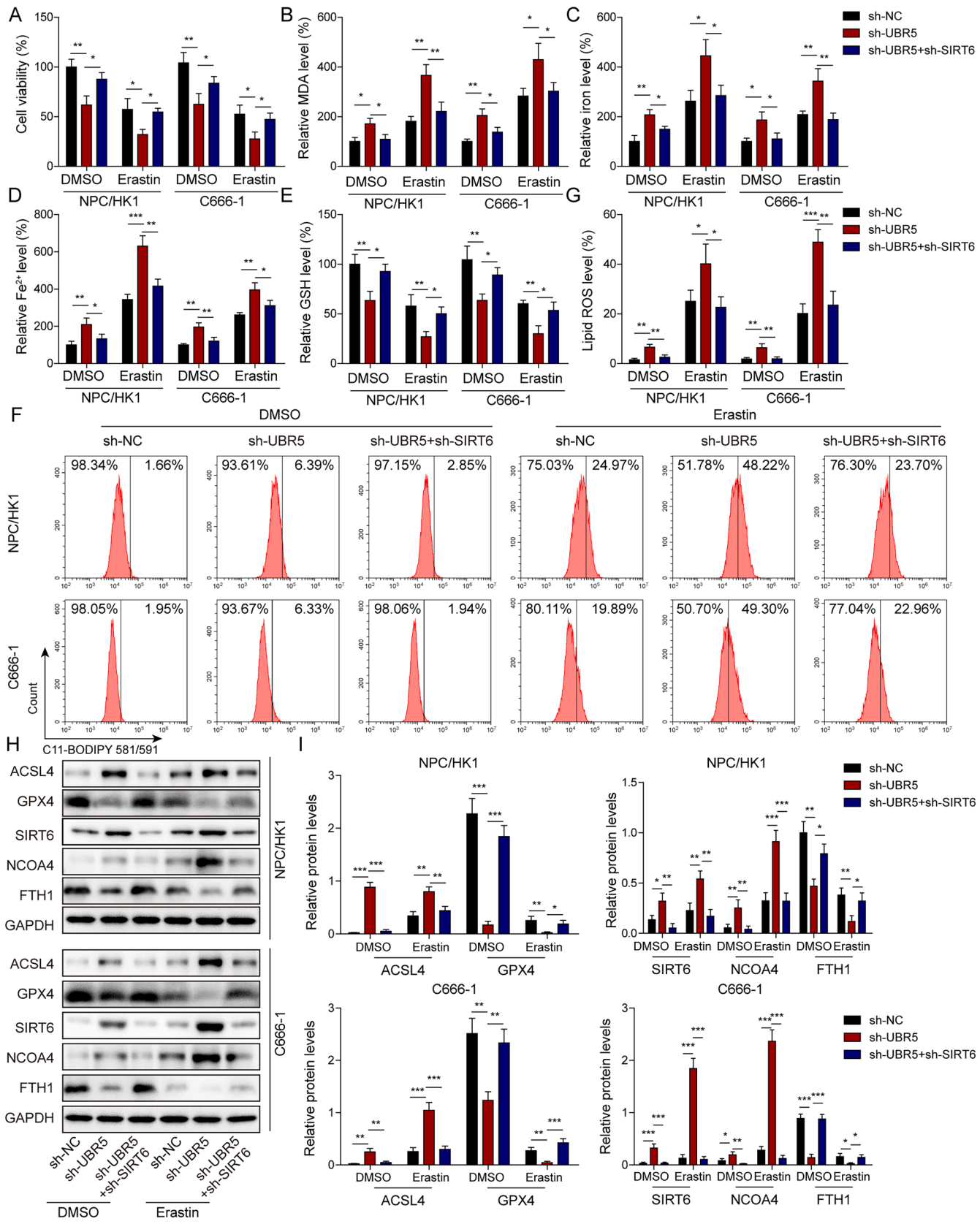

Fig. 7. UBR5 suppressed ferroptosis through SIRT6 in NPC cells. NPC/HK1 and C666-1 cells transfected with sh-NC, sh-UBR5 or sh-UBR5 + sh-SIRT6 were treated with Erastin at 10 μM. DMSO was used as the solvent control. (A) Cell viability was evaluated with CCK-8 after Erastin (10 μM) treatment. Relative MDA (B), total iron (C), Fe^{2+} (D), and GSH (E) in NPC/HK1 and C666-1 cells after Erastin (10 μM) treatment. (F and G) Measurement of lipid peroxidation by flow cytometry after Erastin (10 μM) treatment. (H and I) Western blotting analysis of ACSL4, GPX4, SIRT6, NCOA4, FTH1 and GAPDH after Erastin (10 μM) treatment. * $p < 0.05$, ** $p < 0.01$ and *** $p < 0.001$.

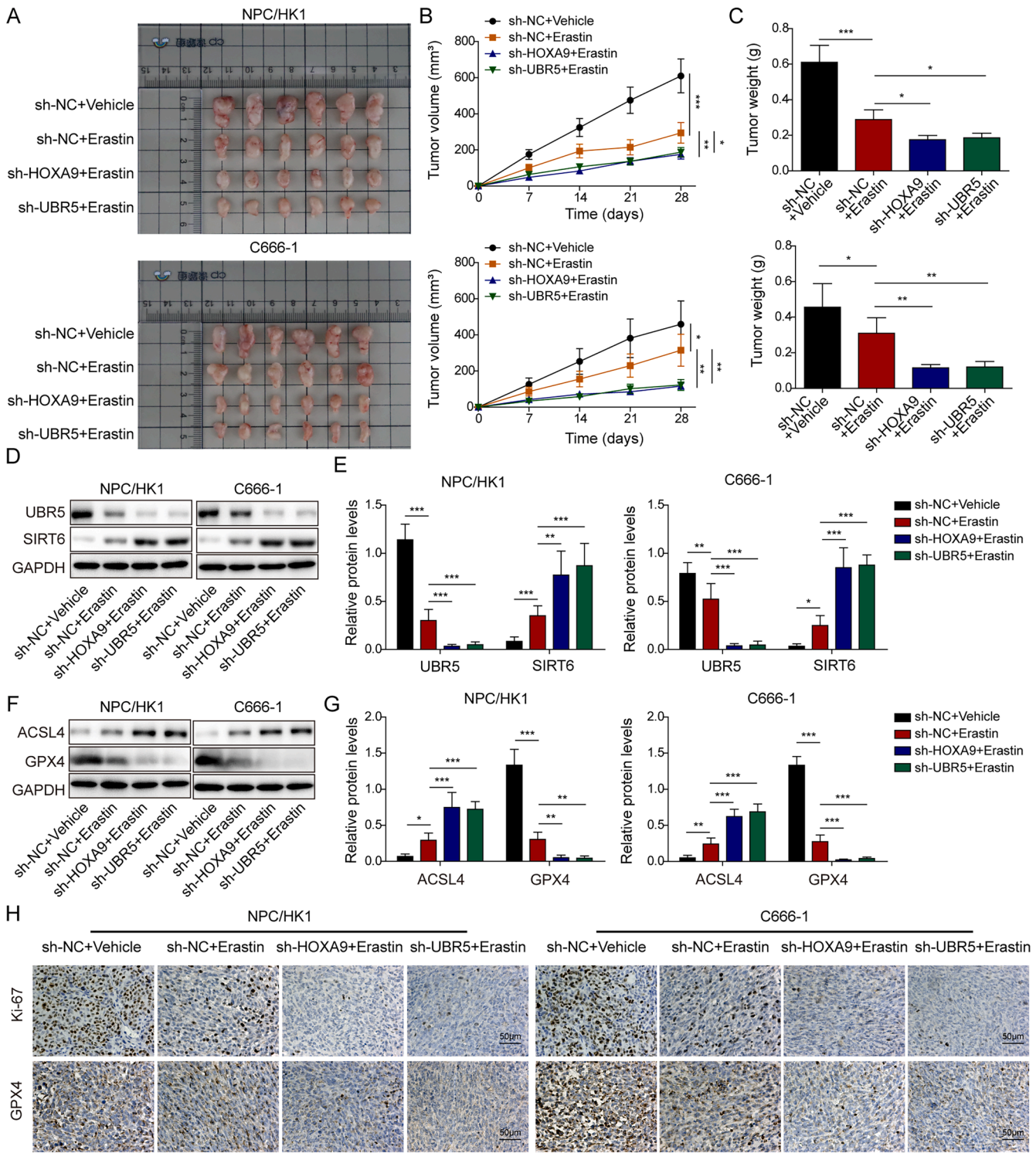

Fig. 8. Knockdown of HOXA9 or UBR5 promoted ferroptosis through SIRT6 and repressed NPC growth in mice. NPC/HK1 and C666-1cells were lentivirally transfected with sh-NC, sh-HOXA9 or sh-UBR5 and subsequently subcutaneously injected into mice. Mice were administrated with vehicle or Erastin. (A) Photos of excised subcutaneous tumors. (B) Tumor volume (n = 6 per group). (C) Tumor weight (n = 6 per group). (D and E) Protein levels of UBR5 and SIRT6 in tumor tissues. (F and G) Protein levels of ACSL4 and GPX4 in tumor tissues. (H) IHC staining of Ki-67 and GPX4 (Scale bar, 50 μm). * $p < 0.05$, ** $p < 0.01$ and *** $p < 0.001$.

A previous study reported that sirtuin could be stabilized by GSK3β through decoupling UBR5 [66]. Silencing of SIRT6 promoted ferroptosis to sensitizing gastric cancer cells to sorafenib [25]. These studies indicated us that SIRT6 might be targeted by UBR5 to participate in the regulation of ferroptosis in NPC. Indeed, we found that UBR5 promoted ubiquitination and degradation of SIRT6 to reduce ferroptosis sensitivity of NPC cells, and overexpression of SIRT6 enhanced ferroptosis in NPC cells.

Regarding the mechanism linking SIRT6 and GPX4, we did not further investigate it. A previous study reported that inhibition of SIRT6 caused KEAP1 upregulation, which in turn degraded NRF2 and downregulated GPX4, suggesting that SIRT6 promoted GPX4 expression [25]. However, we observed increased SIRT6 expression but decreased GPX4 expression in NPC cells. Therefore, SIRT6-mediated downregulation of

GPX4 in this study may not be attributed to the KEAP1/Nrf2 axis. As previously reported, SIRT6 is a regulator of the NCOA4/FTH1 axis [28]. Yang et al. reported that overexpression of SIRT6 increased the ratio of LC3B II/I and promoted the expression of NCOA4 but suppressed the expression of p62 and FTH, indicating the activation of NCOA4-dependent autophagy [26]. We found that SIRT6 overexpression enhanced NCOA4 expression but reduced FTH1 expression. Their expression change suggested the possibility that SIRT6/NCOA4/FTH1 might be implicated in the regulation of GPX4 or ACSL4, but it needs further investigation in future studies.

Collectively, we demonstrated that O-GlcNAc-modified HOXA9 suppressed ferroptosis by enhancing UBR5 expression and ubiquitination and degradation of SIRT6, thus promoting NPC progression, supporting the notion that targeting ferroptosis shows great potential in cancer treatment. Our study sheds lights on the regulation of ferroptosis in NPC and highlights the HOXA9-UBR5-SIRT6 axis as therapeutic targets for NPC.

Ethics approval and consent to participate

Patients provided written consent, and our study was approved by the Ethics Committee of Hunan Cancer Hospital. Animal procedures complied with National Institutes of Health guidelines and approved by the Animal Care and Use Committee of Hunan Cancer Hospital.

Consent for publication

The informed consent was obtained from study participants.

Availability of data and materials

The datasets generated during and/or analyzed during the current study are available from the corresponding author on reasonable request.

Funding

This work was supported by Grants from the National Natural Science Foundation of China (Grant No. 82173201, 82272758), the Key Research and Development Program of Hunan Province (No. 2023DK2001,2024DK2007), the Natural Science Foundation of Hunan Province (No.2023JJ4041, 2024JJ9246,2025JJ20099), Scientific Research Project of Hunan Provincial Health Commission (A202302088151, B202304127661), the Hunan Provincial Science and Technology Department(No.2023ZJ1125), Hunan Provincial Health High-Level Talent Scientific Research Project (No.R2023057), National Key Clinical Specialty Scientific Research Project (No. Z2023025).

CRediT authorship contribution statement

Huai Liu: Conceptualization, Visualization, Writing – original draft. **Yingzhou Fu:** Conceptualization, Data curation, Methodology. **Ling Tang:** Conceptualization, Project administration, Validation. **Bo Song:** Investigation. **Wangning Gu:** Resources. **Hongmin Yang:** Supervision. **Tengfei Xiao:** Formal analysis. **Hui Wang:** Writing – review & editing. **Pan Chen:** Funding acquisition, Writing – review & editing.

Declaration of competing interest

The authors declare that they have no known competing financial interests or personal relationships that could have appeared to influence the work reported in this paper.

Acknowledgements

Not applicable.

Supplementary materials

Supplementary material associated with this article can be found, in the online version, at doi:10.1016/j.neo.2025.101142.

References

[1] S.M. Cao, M.J. Simons, C.N. Qian, The prevalence and prevention of nasopharyngeal carcinoma in China, Chin. J. Cancer 30 (2) (2011) 114–119.
[2] D.E. Spratt, N. Lee, Current and emerging treatment options for nasopharyngeal carcinoma, Onco Targets. Ther. 5 (2012) 297–308.
[3] H. Liu, L. Tang, Y. Li, W. Xie, L. Zhang, H. Tang, T. Xiao, H. Yang, W. Gu, H. Wang, et al., Nasopharyngeal carcinoma: current views on the tumor microenvironment's impact on drug resistance and clinical outcomes, Mol. Cancer 23 (1) (2024) 20.
[4] A.W. Lee, B.B. Ma, W.T. Ng, A.T. Chan, Management of nasopharyngeal carcinoma: current practice and future perspective, J. Clin. Oncol.: Official J. Am. Society Clin. Oncol. 33 (29) (2015) 3356–3364.
[5] X.X. Xiang, Y.L. Liu, Y.F. Kang, X. Lu, K. Xu, MEX3A promotes nasopharyngeal carcinoma progression via the miR-3163/SCIN axis by regulating NF-kappaB signaling pathway, Cell Death Dis. 13 (4) (2022) 420.
[6] H. Liu, L. Tang, S. Gong, T. Xiao, H. Yang, W. Gu, H. Wang, P. Chen, USP7 inhibits the progression of nasopharyngeal carcinoma via promoting SPLUNC1-mediated M1 macrophage polarization through TRIM24, Cell Death Dis. 14 (12) (2023) 852.
[7] S.J. Dixon, K.M. Lemberg, M.R. Lamprecht, R. Skouta, E.M. Zaitsev, C.E. Gleason, D.N. Patel, A.J. Bauer, A.M. Cantley, W.S. Yang, et al., Ferroptosis: an iron-dependent form of nonapoptotic cell death, Cell 149 (5) (2012) 1060–1072.
[8] J. Li, F. Cao, H.L. Yin, Z.J. Huang, Z.T. Lin, N. Mao, B. Sun, G. Wang, Ferroptosis: past, present and future, Cell Death Dis. 11 (2) (2020) 88.
[9] C.M. Bebber, F. Muller, L. Prieto Clemente, J. Weber, S: von Karstedt, Ferroptosis in cancer cell biology, Cancers (Basel) 12 (1) (2020).
[10] X. Chen, R. Kang, G. Kroemer, D. Tang, Broadening horizons: the role of ferroptosis in cancer, Nat. Rev. Clin. Oncol. 18 (5) (2021) 280–296.
[11] H.L. Li, N.H. Deng, J.X. Xiao, He XS: Cross-link between ferroptosis and nasopharyngeal carcinoma: New approach to radiotherapy sensitization, Oncol. Lett. 22 (5) (2021) 770.
[12] Y. Xu, Q. Wang, X. Li, Y. Chen, G. Xu, Itraconazole attenuates the stemness of nasopharyngeal carcinoma cells via triggering ferroptosis, Environ. Toxicol. 36 (2) (2021) 257–266.
[13] S. Huang, B. Cao, J. Zhang, Y. Feng, L. Wang, X. Chen, H. Su, S. Liao, J. Liu, J. Yan, et al., Induction of ferroptosis in human nasopharyngeal cancer cells by cucurbitacin B: molecular mechanism and therapeutic potential, Cell Death Dis. 12 (3) (2021) 237.
[14] F. Liu, L. Tang, H. Liu, Y. Chen, T. Xiao, W. Gu, H. Yang, H. Wang, P. Chen, Cancer-associated fibroblasts secrete FGF5 to inhibit ferroptosis to decrease cisplatin sensitivity in nasopharyngeal carcinoma through binding to FGFR2, Cell Death Dis. 15 (4) (2024) 279.
[15] R. Krumlauf, Hox genes in vertebrate development, Cell 78 (2) (1994) 191–201.
[16] E. Eklund, The role of Hox proteins in leukemogenesis: insights into key regulatory events in hematopoiesis, Crit. Rev. Oncog. 16 (1-2) (2011) 65–76.
[17] S.Y. Ko, N. Barengo, A. Ladanyi, J.S. Lee, F. Marini, E. Lengyel, H. Naora, HOXA9 promotes ovarian cancer growth by stimulating cancer-associated fibroblasts, J. Clin. Invest. 122 (10) (2012) 3603–3617.
[18] L. Zhou, Y. Wang, M. Zhou, Y. Zhang, P. Wang, X. Li, J. Yang, H. Wang, Z. Ding, HOXA9 inhibits HIF-1alpha-mediated glycolysis through interacting with CRIP2 to repress cutaneous squamous cell carcinoma development, Nat. Commun. 9 (1) (2018) 1480.
[19] T. Liu, C. Ji, Y. Sun, W. Bai, HOXA9 Expression is associated with advanced tumour stage and prognosis in nasopharyngeal carcinoma, Cancer Manage. Res. 13 (2021) 4147–4154.
[20] Q. Zhu, H. Zhou, L. Wu, Z. Lai, D. Geng, W. Yang, J. Zhang, Z. Fan, W. Qin, Y. Wang, et al., O-GlcNAcylation promotes pancreatic tumor growth by regulating malate dehydrogenase 1, Nat. Chem. Biol. 18 (10) (2022) 1087–1095.
[21] J.B. Lee, K.H. Pyo, H.R. Kim, Role and Function of O-GlcNAcylation in Cancer, Cancers (Basel) (21) (2021) 13.
[22] F. Yu, Q. Zhang, H. Liu, J. Liu, S. Yang, X. Luo, W. Liu, H. Zheng, Q. Liu, Y. Cui, et al., Dynamic O-GlcNAcylation coordinates ferritinophagy and mitophagy to activate ferroptosis, Cell Discov. 8 (1) (2022) 40.
[23] S. Ghosh, Z. Zhou, SIRTain regulators of premature senescence and accelerated aging, Protein Cell 6 (5) (2015) 322–333.
[24] L. Ouyang, L. Yi, J. Li, S. Yi, S. Li, P. Liu, X. Yang, SIRT6 overexpression induces apoptosis of nasopharyngeal carcinoma by inhibiting NF-kappaB signaling, Onco. Targets Ther. 11 (2018) 7613–7624.
[25] S. Cai, S. Fu, W. Zhang, X. Yuan, Y. Cheng, J. Fang, SIRT6 silencing overcomes resistance to sorafenib by promoting ferroptosis in gastric cancer, Biochem. Biophys. Res. Commun. 577 (2021) 158–164.
[26] Z. Yang, R. Huang, Y. Wang, Q. Guan, D. Li, Y. Wu, T. Liao, Y. Wang, J. Xiang, SIRT6 drives sensitivity to ferroptosis in anaplastic thyroid cancer through NCOA4-dependent autophagy, Am. J. Cancer Res. 13 (2) (2023) 464–474.
[27] D. Ahn, R.K. Ho, Tri-phasic expression of posterior Hox genes during development of pectoral fins in zebrafish: implications for the evolution of vertebrate paired appendages, Dev. Biol. 322 (1) (2008) 220–233.
[28] Y. Mi, C. Wei, L. Sun, H. Liu, J. Zhang, J. Luo, X. Yu, J. He, H. Ge, P. Liu, Melatonin inhibits ferroptosis and delays age-related cataract by regulating SIRT6/p-Nrf2/

GPX4 and SIRT6/NCOA4/FTH1 pathways, Biomed. PharmacOther 157 (2023) 114048.
[29] R.F. Shearer, M. Iconomou, C.K. Watts, D.N. Saunders, Functional Roles of the E3 Ubiquitin Ligase UBR5 in Cancer, Mol. Cancer Res.: MCR 13 (12) (2015) 1523–1532.
[30] F. Ding, X. Zhu, X. Song, P. Yuan, L. Ren, C. Chai, W. Zhou, X. Li, UBR5 oncogene as an indicator of poor prognosis in gastric cancer, Exp. Ther. Med. 20 (5) (2020) 7.
[31] G.T. Chung, R.W. Lung, A.B. Hui, K.Y. Yip, J.K. Woo, C. Chow, C.Y. Tong, S.D. Lee, J.W. Yuen, S.W. Lun, et al., Identification of a recurrent transforming UBR5-ZNF423 fusion gene in EBV-associated nasopharyngeal carcinoma, J. Pathol. 231 (2) (2013) 158–167.
[32] N. Hassan, H. Yi, B. Malik, L. Gaspard-Boulinc, S.E. Samaraweera, D.A. Casolari, J. Seneviratne, A. Balachandran, T. Chew, A. Duly, et al., Loss of the stress sensor GADD45A promotes stem cell activity and ferroptosis resistance in LGR4/HOXA9-dependent AML, Blood 144 (1) (2024) 84–98.
[33] Q. Lu, X. Zhang, T. Liang, X. Bai, O-GlcNAcylation: an important post-translational modification and a potential therapeutic target for cancer therapy, Mol. Med. 28 (1) (2022) 115.
[34] Z. Ran, L. Zhang, M. Dong, Y. Zhang, L. Chen, Q. Song, O-GlcNAcylation: a crucial regulator in cancer-associated biological events, Cell Biochem. Biophys. 81 (3) (2023) 383–394.
[35] H. Zhang, J. Zhang, H. Dong, Y. Kong, Y. Guan, Emerging field: O-GlcNAcylation in ferroptosis, Front. Mol. Biosci. 10 (2023) 1203269.
[36] E.P. Tan, S.R. McGreal, S. Graw, R. Tessman, S.J. Koppel, P. Dhakal, Z. Zhang, M. Machacek, N.E. Zachara, D.C. Koestler, et al., Sustained O-GlcNAcylation reprograms mitochondrial function to regulate energy metabolism, J. Biol. Chem. 292 (36) (2017) 14940–14962.
[37] H.M. Itkonen, N. Poulose, R.E. Steele, S.E.S. Martin, Z.G. Levine, D.Y. Duveau, R. Carelli, R. Singh, A. Urbanucci, M. Loda, et al., Inhibition of O-GlcNAc transferase renders prostate cancer cells dependent on CDK9, Mol. Cancer Res.: MCR 18 (10) (2020) 1512–1521.
[38] S. Gong, L. Xiong, Z. Luo, Q. Yin, M. Huang, Y. Zhou, J. Li, SIRT6 promotes ferroptosis and attenuates glycolysis in pancreatic cancer through regulation of the NF-kappaB pathway, Exp. Ther. Med. 24 (2) (2022) 502.
[39] K.C.W. Wong, E.P. Hui, K.W. Lo, W.K.J. Lam, D. Johnson, L. Li, Q. Tao, K.C. A. Chan, K.F. To, A.D. King, et al., Nasopharyngeal carcinoma: an evolving paradigm, Nat. Rev. Clin. Oncol. 18 (11) (2021) 679–695.
[40] A. Hildesheim, C.P. Wang, Genetic predisposition factors and nasopharyngeal carcinoma risk: a review of epidemiological association studies, 2000-2011: rosetta stone for NPC: genetics, viral infection, and other environmental factors, Semin. Cancer Biol. 22 (2) (2012) 107–116.
[41] L. Wu, C. Li, L. Pan, Nasopharyngeal carcinoma: a review of current updates, Exp. Ther. Med. 15 (4) (2018) 3687–3692.
[42] T. Li, X. Guo, M. Ji, F. Li, H. Wang, W. Cheng, H. Chen, M. Ng, S. Ge, Y. Yuan, et al., Establishment and validation of a two-step screening scheme for improved performance of serological screening of nasopharyngeal carcinoma, Cancer Med. 7 (4) (2018) 1458–1467.
[43] C. Xie, H. Li, Y. Yan, S. Liang, Y. Li, L. Liu, C. Cui, Y. Liu, A nomogram for predicting distant metastasis using nodal-related features among patients with nasopharyngeal carcinoma, Front. Oncol. 10 (2020) 616.
[44] M. Jiang, M. Qiao, C. Zhao, J. Deng, X. Li, C. Zhou, Targeting ferroptosis for cancer therapy: exploring novel strategies from its mechanisms and role in cancers, Transl. Lung Cancer Res. 9 (4) (2020) 1569–1584.
[45] B. Lu, X.B. Chen, M.D. Ying, Q.J. He, J. Cao, B. Yang, The role of ferroptosis in cancer development and treatment response, Front. Pharmacol. 8 (2017) 992.
[46] X. Chen, P.B. Comish, D. Tang, R. Kang, Characteristics and biomarkers of ferroptosis, Front. Cell Dev. Biol. 9 (2021) 637162.
[47] L. Yuan, S. Li, Q. Chen, T. Xia, D. Luo, L. Li, S. Liu, S. Guo, L. Liu, C. Du, et al., EBV infection-induced GPX4 promotes chemoresistance and tumor progression in nasopharyngeal carcinoma, Cell Death Differ. (2022).
[48] W. Zhang, X. Li, J. Xu, Y. Wang, Z. Xing, S. Hu, Q. Fan, S. Lu, J. Cheng, J. Gu, et al., The RSL3 induction of KLK lung adenocarcinoma cell ferroptosis by inhibition of USP11 activity and the NRF2-GSH Axis, Cancers (Basel) 14 (21) (2022).
[49] S. Jang, X.R. Chapa-Dubocq, Y.Y. Tyurina, C.M. St Croix, A.A. Kapralov, V. A. Tyurin, H. Bayir, V.E. Kagan, S. Javadov, Elucidating the contribution of mitochondrial glutathione to ferroptosis in cardiomyocytes, Redox Biol. 45 (2021) 102021.
[50] D.M. Cheff, C. Huang, K.C. Scholzen, R. Gencheva, M.H. Ronzetti, Q. Cheng, M. D. Hall, E.S.J. Arner, The ferroptosis inducing compounds RSL3 and ML162 are not direct inhibitors of GPX4 but of TXNRD1, Redox Biol. 62 (2023) 102703.
[51] P.K. Mandal, A. Seiler, T. Perisic, P. Kolle, A. Banjac Canak, H. Forster, N. Weiss, E. Kremmer, M.W. Lieberman, S. Bannai, et al., System x(c)- and thioredoxin reductase 1 cooperatively rescue glutathione deficiency, J. Biol. Chem. 285 (29) (2010) 22244–22253.
[52] S.Y. Ko, H. Naora, HOXA9 promotes homotypic and heterotypic cell interactions that facilitate ovarian cancer dissemination via its induction of P-cadherin, Mol. Cancer 13 (2014) 170.
[53] K.Y. Chung, G. Morrone, J.J. Schuringa, M. Plasilova, J.H. Shieh, Y. Zhang, P. Zhou, M.A. Moore, Enforced expression of NUP98-HOXA9 in human CD34(+) cells enhances stem cell proliferation, Cancer Res. 66 (24) (2006) 11781–11791.
[54] S. Chen, J. Yu, X. Lv, L. Zhang, HOXA9 is critical in the proliferation, differentiation, and malignancy of leukaemia cells both in vitro and in vivo, Cell Biochem. Funct. 35 (7) (2017) 433–440.
[55] T. Issad, H. Al-Mukh, A. Bouaboud, P. Pagesy, Protein O-GlcNAcylation and the regulation of energy homeostasis: lessons from knock-out mouse models, J. Biomed. Sci. 29 (1) (2022) 64.
[56] T. Song, Q. Zou, Y. Yan, S. Lv, N. Li, X. Zhao, X. Ma, H. Liu, B. Tang, L. Sun, DOT1L O-GlcNAcylation promotes its protein stability and MLL-fusion leukemia cell proliferation, Cell Rep. 36 (12) (2021) 109739.
[57] X. Yang, K. Qian, Protein O-GlcNAcylation: emerging mechanisms and functions, Nat. Rev. Mol. Cell Biol. 18 (7) (2017) 452–465.
[58] G. Zhu, A. Murshed, H. Li, J. Ma, N. Zhen, M. Ding, J. Zhu, S. Mao, X. Tang, L. Liu, et al., O-GlcNAcylation enhances sensitivity to RSL3-induced ferroptosis via the YAP/TFRC pathway in liver cancer, Cell Death Dis. 7 (1) (2021) 83.
[59] C.T. Collins, J.L. Hess, Deregulation of the HOXA9/MEIS1 axis in acute leukemia, Curr. Opin. Hematol. 23 (4) (2016) 354–361.
[60] Y. Jin, H.K. Kim, J. Lee, E.Y. Soh, J.H. Kim, I. Song, Y.S. Chung, Y.J. Choi, Transcription factor HOXA9 is linked to the calcification and invasion of papillary thyroid carcinoma, Sci. Rep. 9 (1) (2019) 6773.
[61] S. Koyuncu, I. Saez, H.J. Lee, R. Gutierrez-Garcia, W. Pokrzywa, A. Fatima, T. Hoppe, D. Vilchez, The ubiquitin ligase UBR5 suppresses proteostasis collapse in pluripotent stem cells from Huntington's disease patients, Nat. Commun. 9 (1) (2018) 2886.
[62] K.M. Mann, J.M. Ward, C.C. Yew, A. Kovochich, D.W. Dawson, M.A. Black, B. T. Brett, T.E. Sheetz, A.J. Dupuy, I. Australian Pancreatic Cancer Genome, et al., Sleeping beauty mutagenesis reveals cooperating mutations and pathways in pancreatic adenocarcinoma, Proc. Natl. Acad. Sci. U S. A 109 (16) (2012) 5934–5941.
[63] J. Li, W. Zhang, J. Gao, M. Du, H. Li, M. Li, H. Cong, Y. Fang, Y. Liang, D. Zhao, et al., E3 ubiquitin ligase UBR5 promotes the metastasis of pancreatic cancer via destabilizing F-actin capping protein CAPZA1, Front. Oncol. 11 (2021) 634167.
[64] T. Gudjonsson, M. Altmeyer, V. Savic, L. Toledo, C. Dinant, M. Grofte, J. Bartkova, M. Poulsen, Y. Oka, S. Bekker-Jensen, et al., TRIP12 and UBR5 suppress spreading of chromatin ubiquitylation at damaged chromosomes, Cell 150 (4) (2012) 697–709.
[65] A.A. Sarshad, M. Corcoran, B. Al-Muzzaini, L. Borgonovo-Brandter, A. Von Euler, D. Lamont, N. Visa, P. Percipalle, Glycogen synthase kinase (GSK) 3beta phosphorylates and protects nuclear myosin 1c from proteasome-mediated degradation to activate rDNA transcription in early G1 cells, PLoS Genet. 10 (6) (2014) e1004390.
[66] X. Tang, G. Li, L. Shi, F. Su, M. Qian, Z. Liu, Y. Meng, S. Sun, J. Li, B. Liu, Combined intermittent fasting and ERK inhibition enhance the anti-tumor effects of chemotherapy via the GSK3beta-SIRT7 axis, Nat. Commun. 12 (1) (2021) 5058.